A&A 476, 73–81 (2007)
DOI: 10.1051/0004-6361:20078187

Astronomy & Astrophysics

A new calibration of Galactic Cepheid period-luminosity relations from B to K bands, and a comparison to LMC relations⋆

P. Fouqué[1], P. Arriagada[1,4], J. Storm[2], T. G. Barnes[5,9], N. Nardetto[3], A. Mérand[8], P. Kervella[7], W. Gieren[6], D. Bersier[10], G. F. Benedict[5], and B. E. McArthur[5]

[1] Observatoire Midi-Pyrénées, Laboratoire d'Astrophysique, UMR 5572, Université Paul Sabatier - Toulouse 3, 14 avenue Edouard Belin, 31400 Toulouse, France
e-mail: pfouque@ast.obs-mip.fr
[2] Astrophysikalisches Institut Potsdam, An der Sternwarte 16, 14482 Potsdam, Germany
[3] Max-Planck-Institut für Radioastronomie, Infrared Interferometry Group, Auf dem Hügel 69, 53121 Bonn, Germany
[4] Departamento de Astronomía y Astrofísica, Pontificia Universidad Católica de Chile, Campus San Joaquín, Vicuña Mackenna 4860, Casilla 306, Santiago 22, Chile
[5] University of Texas at Austin, McDonald Observatory, 1 University Station, C1402, Austin, TX 78712-0259, USA
[6] Universidad de Concepción, Departamento de Física, Grupo de Astronomía, Casilla 160-C, Concepción, Chile
[7] Observatoire de Paris-Meudon, LESIA, UMR 8109, 5 place Jules Janssen, 92195 Meudon Cedex, France
[8] Center for High Angular Resolution Astronomy, Georgia State University, PO Box 3965, Atlanta, Georgia 30302-3965, USA
[9] currently on assignment to the National Science Foundation, 4201 Wilson Boulevard, Arlington, VA 22230, USA
[10] Astrophysics Research Institute, Liverpool John Moores University, Twelve Quays House, Egerton Wharf, Birkenhead, CH41 1LD, UK

Received 29 June 2007 / Accepted 15 September 2007

ABSTRACT

Context. The universality of the Cepheid period-luminosity (*PL*) relations has been under discussion since metallicity effects were assumed to play a role in the value of the intercept and, more recently, of the slope of these relations.
Aims. The goal of the present study is to calibrate the Galactic *PL* relations in various photometric bands (from B to K) and to compare the results to the well-established *PL* relations in the LMC.
Methods. We use a set of 59 calibrating stars, the distances of which are measured using five different distance indicators: Hubble Space Telescope and revised Hipparcos parallaxes, infrared surface brightness and interferometric Baade-Wesselink parallaxes, and classical Zero-Age-Main-Sequence-fitting parallaxes for Cepheids belonging to open clusters or OB stars associations. A detailed discussion of absorption corrections and projection factor to be used is given.
Results. We find no significant difference in the slopes of the *PL* relations between LMC and our Galaxy.
Conclusions. We conclude that the Cepheid *PL* relations have universal slopes in all photometric bands, not depending on the galaxy under study (at least for LMC and Milky Way). The possible zero-point variation with metal content is not discussed in the present work, but an upper limit of 18.50 for the LMC distance modulus can be deduced from our data.

Key words. stars: variables: Cepheids – stars: distances – stars: fundamental parameters – galaxies: distances and redshifts

1. Introduction

Soon after the release of Hipparcos measurements of Cepheid parallaxes (Perryman & ESA 1997), Feast & Catchpole (1997) intended to re-calibrate the Period-Luminosity relation of Cepheids using these parallaxes, with a conflictual result on the distance to the Large Magellanic Cloud. However, the accuracy of the zero-point was quite limited for such distant stars, and the derived LMC modulus depended heavily on the adopted PL slope.

Later, Benedict et al. (2002) obtained a parallax for δ Cep, using the Fine Guidance Sensor 3 instrument on board HST, with an accuracy of 4%, already better than the most accurate Cepheid parallax from Hipparcos (α UMi, 6%). Recently, Benedict et al. (2007) managed to measure 9 additional Cepheid parallaxes, using FGS 1r on HST, with a mean accuracy of 8%.

Finally, van Leeuwen et al. (2007) published a revision of Hipparcos parallaxes, with a typical improvement in accuracy for Cepheids of a factor two. α UMi is back at the top place, with an accuracy of 1.6%. But the second star, δ Cep, still has an accuracy slightly worse than the HST measurement (5.2% vs. 4.1%).

In parallel, Cepheid distances estimated via several variants of the Baade-Wesselink method have been secured. We use here two of these variants, the Infra-Red Surface Brightness technique (hereafter, IRSB) (e.g.: Fouqué & Gieren 1997) and the Interferometric Baade-Wesselink method (IBW), where Cepheid pulsation is directly measured with a long-baseline interferometer (see, e.g.: Kervella et al. 2004b). The random uncertainty of distances obtained via these techniques is very small (~3%), but systematic uncertainties hamper a reliable calibration from this method alone. This mainly comes from uncertainty in the so-called projection factor, which converts observed radial velocities to pulsation velocities. A recent discussion about which factor should be applied to these two techniques (IBW and

⋆ Tables 2, 6 and 7 are only available in electronic form at http://www.aanda.org

Table 1. Adopted conversion relations for extinction values, transforming $E(B-V)$ (X) to the Laney & Caldwell (2007) system, by $E(B-V)$ (L07) = $a\ E(B-V)$ (X) + b.

Authors	F95 id	slope	intercept	σ	N	weight
Parsons & Bell (1975)	PB	0.908 ± 0.026		0.064	105	0.3
Yakimova et al. (1975)	YT	0.863 ± 0.017	0.036 ± 0.007	0.034	82	1.2
Janot-Pacheco (1976)	JP	0.873 ± 0.077		0.089	30	0.1
Dean et al. (1978)	DWC	0.961 ± 0.012	−0.014 ± 0.005	0.025	77	3.2
Pel (1978)	PE	0.945 ± 0.029		0.047	64	0.5
Kron & Roach (1979)	KR	0.867 ± 0.028		0.072	124	0.2
Feltz & McNamara (1980)	FM	0.890 ± 0.022	0.039 ± 0.013	0.046	54	0.6
Dean (1981)	DE	0.857 ± 0.034		0.038	35	0.9
Turner et al. (1987)	TLE	0.938 ± 0.050		0.037	21	1.0
Schechter et al. (1992)	SACK	0.861 ± 0.073	0.039 ± 0.037	0.034	9	1.2
Laney & Stobie (1993)	LS	0.985 ± 0.008		0.015	45	-
Fernie et al. (1995)	FE	0.952 ± 0.010		0.029	147	1.9
Eggen (1996)	EG2	0.754 ± 0.045	0.064 ± 0.013	0.043	34	0.7
Bersier (2002)		0.883 ± 0.021	0.035 ± 0.009	0.040	64	0.8

IRSB) can be found in Nardetto et al. (2004). This study, based on a hydrodynamical model of δ Cep has been then confirmed observationally by Mérand et al. (2005) using the accurate distance measurement of this star by the HST.

Finally, the standard technique of deriving Cepheid distances from their association with an open cluster is still valid (see, e.g.: Tammann et al. 2003) and will also be discussed here.

Our goal is to calibrate the *PL* relation in various photometric bands (from B to K) using Galactic Cepheids of known distances, and to compare the resulting relations to those in the Large Magellanic Cloud (LMC).

2. Observables

2.1. Photometry

For a Cepheid to enter our sample, we request photometry at least in B, V, I_c, J and K bands. We use the catalogue from Berdnikov et al. (2000) for the visible photometry, supplemented in a few cases by data from Sandage et al. (2004) and Groenewegen (1999). These are intensity-mean values.

For the near-infrared bands, we started from the Berdnikov et al. (1996a) catalogue. However, it does not include more recent measurements (Barnes et al. 1997), and it is not in a well-defined system, although it claims to be in the CIT system.

We therefore decided to use original intensity-mean values from Welch et al. (1984), Laney & Stobie (1992), Barnes et al. (1997) and to convert them to the 2MASS system (Skrutskie et al. 2006), which is the only near-infrared system covering the whole sky. Transformations from CIT and SAAO systems to 2MASS use the updated conversion relations from 2MASS web site[1], which replace the original Carpenter's equations (Carpenter 2001). When several sources are available, we take a weighted average of transformed intensity-mean values, using the number of measurements as a weight. When only Berdnikov et al. (1996a) values are available, we did not go back to the original publication and assume that they are in the CIT system to convert them accordingly. If the intensity-mean values were not available from the original source (case of Barnes et al. 1997 and Y Sgr in Welch et al. 1984), we used the values as published in Groenewegen (1999) (SAAO system) and the corresponding conversion. All these recipes obviously limit the accuracy of the resulting magnitudes, but we have to live with it, as measuring good near-infrared light curves of bright stars is difficult nowadays.

2.2. Absorption

2.2.1. Extinction

To correct observed magnitudes in each band for galactic absorption, we need an estimate of the extinction E(B-V) and a reddening law. Tammann et al. (2003) (hereafter T03) discuss these issues in details: they first adopt a revised Fernie's system (Fernie et al. 1995) (hereafter F95) by converting extinction values from various authors in Fernie's David Dunlap Observatory database of Galactic Classical Cepheids[2] to Fernie's own measurements system, before averaging them. Then, they test for a possible scale error of this mean system and indeed detect that the mean F95 extinctions are too large by ∼5%.

In the present work, we make use of the recently published Laney & Caldwell (2007) (hereafter L07) extinction values, based on $B\ V\ I_c$ photometry. A test of these extinctions (solar metallicity assumed for all stars) vs. Fernie's original system (columns FE1 and FE2 in his database, FE1 if both present) for 155 stars in common reveals that the L07 values are precisely on the corrected T03 system (see their Eq. (2) and Table 1).

We therefore adopt the L07 system as reference, and convert available data of each reference in Fernie's database using relations in Table 1, where the symbols correspond to the column headings in the database. We replace values from Bersier (1996) by the revised and more extensive data set published in Bersier (2002). Note that we adopt only a scale factor when the intercept of the linear relation is not larger than its uncertainty. Also note that we use the direct least-squares relation for conversion, which is the one giving unbiased results. This explains why all the slopes are smaller than 1.

We then adopt a weighted mean of the individual measurements corrected with the above formulae, with the weights computed as the square inverse of the typical uncertainty of a given source, derived from the above rms dispersions: we assume for instance that L07 and DWC equally contribute to the observed dispersion of their conversion relation, giving 0.018 uncertainty to each, corresponding to a weight of 3.2 each. We do not use the LS values in the mean, which probably correspond to older

[1] www.ipac.caltech.edu/2mass/releases/allsky/doc/sec6_4b.html

[2] www.astro.utoronto.ca/DDO/research/cepheids/table_colourexcess.html

Table 3. Comparaison of published total-to-selective absorption ratios in various bands.

Filter	$R(\lambda)$	Reference
V	3.26	Berdnikov et al. (1996b)
V	3.30	Fouqué et al. (2003)
V	3.23	Sandage et al. (2004)
V	3.1	Benedict et al. (2007)
V	3.23	this work
I_c	1.86	Berdnikov et al. (1996b)
I_c	1.99	Fouqué et al. (2003)
I_c	1.95	Sandage et al. (2004)
I_c	1.73	Benedict et al. (2007)
I_c	1.96	this work
J	0.82	Fouqué et al. (2003)
J	0.88	Benedict et al. (2007)
J	0.94	this work
H	0.48	Fouqué et al. (2003)
H	0.58	this work
K	0.30	Fouqué et al. (2003)
K	0.34	Benedict et al. (2007)
K_s	0.38	this work

derivations of L07 values. For convenience, we list the results for the whole sample of 158 stars in Table 2.

GT Car, SU Cru and BG Cru do not appear in L07: for GT Car, we use its Schechter et al. (1992) value of extinction from Fernie's database, converted to L07 system using the corresponding equation in Table 1; similarly for SU Cru and BG Cru, we use a weighted mean of their converted values of extinction from Fernie's database and Bersier (2002), after rejection of a discrepant value from Fernie et al. (1995) for BG Cru.

2.2.2. Reddening law

For the reddening law, we adopt the Cardelli et al. (1989) system, contrarily to our previous works, where the reddening law was derived from Laney & Stobie (1993) (hereafter LS93), and Caldwell & Coulson (1987). This is not a matter of preference, but we had to derive absorption ratios for the 2MASS system, and Cardelli's formulae were suitable for this purpose: we adopted isophotal wavelengths from Cohen et al. (2003). For the Cousins bands not given in Cardelli et al. (1989), we used isophotal wavelengths from Bessell et al. (1998). We neglect the small difference with effective wavelengths suitable for Cepheids colours.

Cardelli's formulae depend on the total-to-selective absorption ratio in V band, R_V. This ratio slightly depends on the star colour and on extinction, but, as in Fouqué et al. (2003), we adopt a constant value, because the colour dependency is not well established and in any case small for the colour range of Cepheids. We adopt the mean value derived by Sandage et al. (2004), namely $R_V = 3.23$, and $R_B = R_V + 1$. Table 3 compares published values of these ratios in various bands.

The small isophotal wavelength differences between SAAO and 2MASS systems do not explain the difference in infrared total-to-selective absorption ratios between Fouqué et al. (2003), adopted from LS93, and the present work. The source of this discrepancy is the different approach to derive the reddening law used by Cardelli et al. (1989) and LS93.

Table 4 gives our adopted reddening law for the various photometric bands, and the LS93 values for the SAAO infrared bands.

Table 4. Adopted reddening law from Cardelli et al. (1989), using isophotal wavelengths (in μm) from Bessell et al. (1998) for Cousins bands and from Cohen et al. (2003) for 2MASS bands, and $R_V = 3.23$. For comparison, LS93 values in the SAAO infrared bands are also given.

Filter	λ_{iso}	$A(\lambda)/A(V)$	LS93
B	0.438	1.310	
V	0.545	1	
R_c	0.641	0.845	
I_c	0.798	0.608	
J	1.235	0.292	0.249
H	1.662	0.181	0.147
K_s	2.159	0.119	0.091

2.3. Parallaxes

We will now give some details about the five methods we use to measure Cepheid parallaxes.

2.3.1. Trigonometric parallaxes

We use two sources of trigonometric parallaxes: HST parallaxes, published by Benedict et al. (2002) and Benedict et al. (2007), and the revised Hipparcos parallaxes of Cepheids, from van Leeuwen et al. (2007). Table 1 of the latter reference compares the two sources for the 10 Cepheids measured by HST. It is clear that even for this selected sample of the best revised Hipparcos parallaxes, the HST measurements are slightly superior. The case of Y Sgr, where the discrepancy is much larger than the combined uncertainties, is worrying.

In the present study, we adopt the HST parallaxes as reference, and make use of the revised Hipparcos parallaxes only if their accuracy is better than 30% and they are not common to the HST sample: there are 8 such stars, 5 of them being classified as first overtone pulsator.

2.3.2. IRSB parallaxes

The Infra-Red Surface Brightness technique can give very precise parallaxes when the radial velocity and light curves are well defined. However, they directly depend on the adopted value of the projection factor, which we will discuss in detail here.

For the visible surface brightness versus $(V - K)$ colour relation, we still use Fouqué & Gieren (1997) for consistency with previous work, although it has been superseded by more recent studies. In fact, all the more recent calibrations (Nordgren et al. 2002; Kervella et al. 2004a; Groenewegen 2004), either based on giants or on Cepheids, confirm the validity of this calibration and of the hypothesis that stable giant stars and pulsating Cepheids obey the same relation.

Since the publication of our last paper on IRSB distances in Barnes et al. (2005), which contained 38 Cepheids, many new measurements have been added to our database to reach a total of 70 stars. A separate publication describing these new results and giving references to the spectroscopic and photometric data involved in this work is in preparation (Storm et al. 2008).

The projection factor p is defined as the ratio of the pulsational velocity to the radial velocity. Early studies (e.g.: Carroll 1928) only considered geometrical effects, namely limb darkening and atmospheric expansion at constant velocity, and arrived at values between 1.375 and 1.412 for visible linear limb-darkening coefficients u_V between 0.8 and 0.6, respectively. This is well represented by Eq. (6) in Nardetto et al. (2006),

$p = 1.52-0.18\ u_V$. As the limb darkening is mainly related to the effective temperature and the surface gravity, it varies from one Cepheid to another. We already see that a single p-factor for all Cepheids cannot be but an over-simplistic approximation, and even a single p-factor for a given Cepheid is an approximation, because its temperature and surface gravity vary along the pulsation cycle (for details, see, e.g.: Marengo et al. 2002, 2003).

And this is just the tip of the iceberg: p also depends on the proper amplitude of the pulsation velocity, on the lines under study, on the way the radial velocities are measured, on the spectral resolution, as first shown by Parsons (1972). Following the work of Hindsley & Bell (1986), who adapted the value of p for radial velocities measured through cross-correlation techniques, where many lines are mixed into the measurement of the correlation peak, we adopted as an approximation of all these effects $p = 1.39-0.03 \log P$ to represent the variation of the p-factor with the period of the Cepheid (hereafter $p\,(P)$ relation). This is obviously a rather crude approximation, but it is difficult to be more specific. In Gieren et al. (2005), we revised the coefficients of this relation, because they lead to an apparent variation of the LMC distance with Cepheid period, in a sample of 13 LMC Cepheids for which an IRSB distance was measured. At the same time, the new relation $p = 1.58-0.15 \log P$ leads to a better agreement between LMC and Galactic slopes of the *PL* relations in various photometric bands, raising again the hope of universal *PL* relations. Improvements in the modelling investigations also permit a better understanding of the various components of the p-factor, but they lead to values more in agreement with our old relation (see e.g.: Nardetto et al. 2004). We will test the most recent relation based on these models and high resolution spectroscopic observations, as published in Nardetto et al. (2007), namely $p = 1.366-0.075 \log P$. In the case of suspected first overtone pulsators, we use the observed period to compute the corresponding p-factor, as in our previous studies, not the corrected period of fundamental pulsation.

2.3.3. Interferometric Baade-Wesselink parallaxes

The originality of the Interferometric Baade-Wesselink method compared to the classical IRSB technique is to measure directly the angular amplitude of the pulsation of the star, instead of deducing it from photometric colours. In the last few years, the considerable improvement of the available long-baseline interferometry (LBI) instrumentation has shed a new light on the IBW technique. The first interferometric observations of a Cepheid were obtained by Mourard et al. (1997), followed by observations from almost all operating interferometers (Lane et al. 2000; Nordgren et al. 2000; Kervella et al. 2001; Kervella et al. 2004c; Mérand et al. 2005; 2006, 2007).

The main difficulty in observing Cepheids by LBI is that they are rare and therefore relatively distant stars. As a consequence, they present small angular sizes, even for the closest ones. The Cepheid which has the largest angular diameter is ℓ Car, with 3 mas, and a baseline of approximately 180 m is already required to fully resolve it in the infrared. As the pulsation amplitude of a Cepheid is about 20% of its size, the detection of the pulsation, necessary to apply the IBW method, is an even more challenging objective. On the 10 nearest Cepheids, an accurate measurement of the amplitude of the pulsation (to a few percent accuracy) requires a baseline length of 150 to 300 m.

As a consequence, the distances to only eight Cepheids have been measured using the true IBW technique: δ Cep (Mérand et al. 2005), η Aql (Lane et al. 2002), β Dor (Kervella et al. 2004c; Davis 2006), ζ Gem (Lane et al. 2002), Y Oph (Mérand et al. 2007), ℓ Car (Kervella et al. 2004b; Davis et al. 2006), W Sgr (Kervella et al. 2004c), and Y Sgr (Mérand 2008). We choose in the present paper to focus on these stars only.

Table 5. Adopted parallaxes measured by the Interferometric Baade-Wesselink technique. The adopted p-factor is listed in the last column.

Star	$\log P$	π	$\sigma(\pi)$	p
η Aql	0.855930	3.31	0.05	1.302
ℓ Car	1.550816	1.90	0.07	1.250
δ Cep	0.729678	3.52	0.10	1.311
β Dor	0.993131	3.05	0.98	1.292
ζ Gem	1.006507	2.91	0.31	1.291
Y Oph	1.233609	2.16	0.08	1.273
W Sgr	0.880522	2.76	1.23	1.300
Y Sgr	0.761428	1.96	0.62	1.309

Before integration, we interpolated the spectroscopic radial velocities using node-constrained cubic splines, as described by Mérand et al. (2007). In the literature, the hypotheses used for the application of the IBW method may substantially differ among authors. In order to get an homogeneous set, we recomputed the parallaxes using the original interferometric uniform disk diameters, a limb-darkening model from Claret (2000), and the p-factor adopted in Sect. 2.3.5. The derived parallaxes are given in Table 5: three of them have large uncertainties and are therefore excluded from the following analysis. The recent discovery of circumstellar envelopes around most Cepheids for which interferometric measures exist (Kervella et al. 2006; Mérand et al. 2006, 2007) has a clear impact on this method, the importance of which must still be assessed.

2.3.4. Open cluster parallaxes

We adopt the parallaxes for Cepheids belonging to open clusters or associations from the recent compilation by Turner & Burke (2002). No correction for the underlying assumed Pleiades distance modulus (5.56) has been attempted, because the validity of such a correction is questionable (Feast 1999). The geometrical parallax of RS Pup is adopted from Sandage et al. (2004).

The basic hypothesis underlying this kind of parallax measurement is that the Cepheid is indeed associated with the cluster. We will see below in Sect. 2.3.5 which Cepheids are dubious members of their association or cluster.

Parallax uncertainties as published by Turner & Burke (2002) seem too small, sometimes reaching 1%. Based on the more realistic uncertainties published by Hoyle et al. (2003), we have set a minimum accuracy of 5%.

2.3.5. Adopted parallaxes

The status of known Cepheid parallaxes is the following, without taking into account Hipparcos parallaxes with a large uncertainty: 81 stars have a parallax from at least one distance indicator, 22 from two, 10 from three, 4 from four, and only 1 from the five distance indicators: see Table 6. Among the 10 stars with HST parallaxes, all have an Hipparcos parallax, 7 have IRSB, 6 have IBW and 2 have ZAMS measurements, but all these measurements largely vary in quality. Moreover, we have to decide about the choice of the final $p\,(P)$ relation to adopt. Obviously, the choice of the slope of the $p\,(P)$ relation with $\log P$ has an influence on the slope of the *PL* relations, in the sense that a shallower slope of this relation (such as the small dependence of the classical relation) leads to a steeper slope in the *PL*

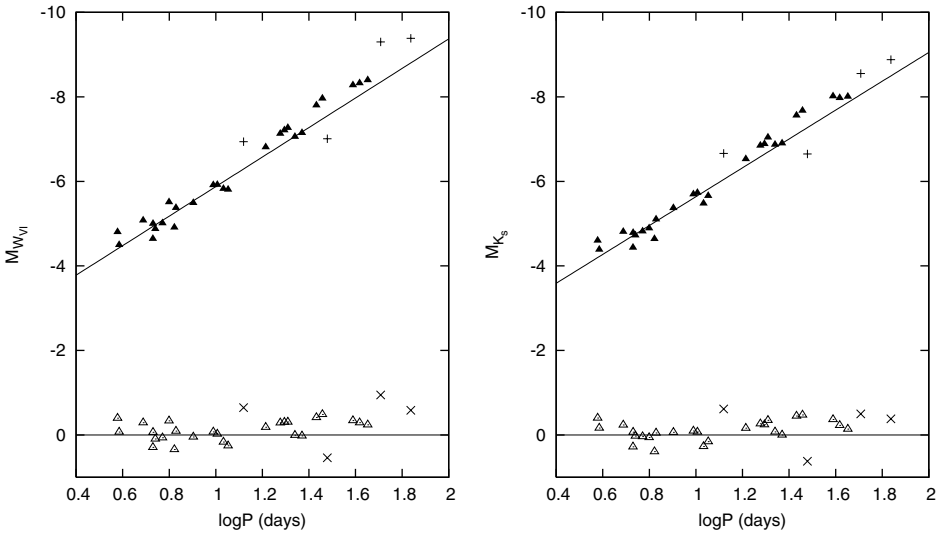

Fig. 1. Comparison of absolute magnitudes derived from ZAMS parallaxes (triangles) for 30 stars with the *PL* relations based on 54 IRSB parallaxes in W_{vi} and K_s bands (solid lines). The bottom panel shows residuals with respect to the IRSB *PL* relations. Long-period Cepheids appear to be progressively shifted. Rejected stars (see text) are marked with pluses and crosses.

relations. On the other hand, there are not enough HST parallaxes to settle this slope definitively (there is only one long-period star in the HST sample).

In Gieren et al. (2005), the slope of the *p (P)* relation with $\log P$ was constrained by individual distance measurements of 13 LMC Cepheids, so that the LMC distance modulus derived from each of these stars did not depend on $\log P$. Although this is a reasonable constraint, a precise determination was hampered by several facts: the period distribution of the Cepheids was not optimal, with all short-period Cepheids belonging to one single cluster, namely NGC 1866; the corrections for the position of each Cepheid with respect to the geometry of the LMC were model-dependent; the uncertainties of the long-period Cepheids distance moduli were too small to explain the observed dispersion of the derived LMC distance moduli among these stars. A revision of this determination with additional stars is in progress. For the time being, we therefore prefer to rely on the slope of the model relation from Nardetto et al. (2007).

However, the zero-point of this relation is only valid for a well-defined way of measuring radial velocities from the observed metallic lines, namely the first moment of the line. As most of our radial velocities come from cross-correlation measurements, where the peak of the cross-correlation is generally measured by a Gaussian fit, there is no reason that the model zero-point applies exactly to these measurements. As we want to use the HST parallaxes as the absolute system, we prefer to determine a preliminary *PL* relation based on IRSB parallaxes, and verify that the zero-point of the *p (P)* relation does not lead to a significant shift of the 10 HST Cepheids when adopting their HST parallaxes. For this purpose, we only use the W_{vi} (see Sect. 3 for definition) and the K_s *PL* relations, as the less dispersed relations being representative of the optical and infrared bands.

We first need to define a clean sample of IRSB calibrators, among the 70 stars with available IRSB parallaxes. After rejection of 5 known first overtone pulsators, of 2 stars with poor data fit, of 3 stars with poor sampling of the K light curve, of 4 additional outliers, and of 2 long-period Cepheids with variable periods, we are left with 54 calibrators. The mean residual of the 10 stars with HST parallaxes from the two *PL* relations is -0.01 ± 0.03 in W_{vi} and -0.05 ± 0.03 in K_s. They are not significant, and we therefore also adopt the zero-point of the model *p (P)* relation from Nardetto et al. (2007).

If we compare the absolute magnitudes in W_{vi} and K_s of the Cepheids using their ZAMS parallaxes to the preliminary *PL* relations based on IRSB parallaxes, we find in a sample of 26 Cepheids[3] a mean shift of -0.09 ± 0.04 mag, corresponding to ZAMS parallaxes being too small by 4%. Part of the explanation of this shift may lie in the assumed Pleiades distance modulus in Turner & Burke (2002), which is 5.56, while the most accurate value given by Soderblom et al. (2005) is 5.63 ± 0.02, a difference of 3%. However, a tendency to get more discrepant parallaxes for long-period Cepheids, as shown in Fig. 1 which displays all 30 stars, leads us not to use the ZAMS parallaxes in the present study. A possible explanation of this effect is that long-period Cepheids are generally assigned to OB associations, where the membership is more difficult to establish. The small shift of ZAMS parallaxes is the most probable explanation to the too large zero-point of the Gieren et al. (2005) *p (P)* relation (1.58), which was adjusted to make IRSB distances correspond to ZAMS ones.

It is interesting to compare the dispersion of the various indicators with respect to the preliminary *PL* relations based on 54 IRSB parallaxes, for which we have 0.15 in K_s and 0.17 in W_{vi}: for the HST, the rms dispersion is 0.10 both in K_s and W_{vi}; for the IBW, it is 0.18 in K_s and 0.21 in W_{vi}, after rejection of Y Oph; and for the ZAMS, it amounts to 0.22 in K_s and 0.23 in W_{vi}, after rejection of GT Car and AQ Pup. Clearly, the HST parallaxes are superior in accuracy to other distance indicators.

We decided not to average parallaxes for a given star among the different techniques, but to use HST parallaxes when available (to be consistent with our adjusted zero-point based on HST system) and IRSB, IBW or revised Hipparcos parallaxes if not. ZAMS parallaxes are not used due to their slight offset. The catalogue of adopted parallaxes is given in Table 6. Suspected first

[3] We have rejected as dubious ZAMS parallaxes of GT Car and AQ Pup, and long-period stars GY Sge and S Vul.

Table 8. Adopted Galactic and LMC *PL* relations: $M = a \log P + b$. Note that intercept error is for the barycenter of data points (no slope error included).

Galaxy	Source	Band	slope a	intercept b	σ	N
MW	this work	B	-2.289 ± 0.091	-0.936 ± 0.027	0.207	58
		V	-2.678 ± 0.076	-1.275 ± 0.023	0.173	58
		R_c	-2.874 ± 0.084	-1.531 ± 0.025	0.180	54
		I_c	-2.980 ± 0.074	-1.726 ± 0.022	0.168	59
		J	-3.194 ± 0.068	-2.064 ± 0.020	0.155	59
		H	-3.328 ± 0.064	-2.215 ± 0.019	0.146	56
		K_s	-3.365 ± 0.063	-2.282 ± 0.019	0.144	58
		W_{vi}	-3.477 ± 0.074	-2.414 ± 0.022	0.168	58
		W_{bi}	-3.600 ± 0.079	-2.401 ± 0.023	0.178	58
LMC	OGLE	B	-2.439 ± 0.046	17.368 ± 0.009	0.239	662
	this work	B	-2.393 ± 0.040	17.356 ± 0.010	0.272	714
	OGLE	V	-2.779 ± 0.031	17.066 ± 0.006	0.160	650
	this work	V	-2.734 ± 0.029	17.052 ± 0.007	0.199	716
	this work	R_c	-2.742 ± 0.060	16.697 ± 0.020	0.185	83
	OGLE	I_c	-2.979 ± 0.021	16.594 ± 0.004	0.107	662
	this work	I_c	-2.957 ± 0.020	16.589 ± 0.005	0.132	692
	Persson	J	-3.153 ± 0.051	16.336 ± 0.015	0.140	92
	this work	J	-3.139 ± 0.026	16.273 ± 0.006	0.128	529
	Persson	H	-3.234 ± 0.042	16.079 ± 0.012	0.116	92
	this work	H	-3.237 ± 0.024	16.052 ± 0.005	0.117	529
	Persson	K_s	-3.281 ± 0.040	16.051 ± 0.011	0.108	92
	this work	K_s	-3.228 ± 0.028	15.989 ± 0.006	0.136	529
	OGLE	W_{vi}	-3.309 ± 0.011	15.875 ± 0.002	0.056	671
	this work	W_{vi}	-3.320 ± 0.011	15.880 ± 0.003	0.070	686
	this work	W_{bi}	-3.454 ± 0.011	15.928 ± 0.003	0.076	688

overtone Cepheids are marked as 'FO' and will not be used in the following calibrations.

3. Galactic Period-Luminosity relations

From the adopted intensity-mean values in the various photometric bands, the extinction value from Table 2, the adopted reddening law from Table 4, and the adopted parallax from Table 6, we derive the absolute magnitudes in B, V, R_c, I_c, J, H and K_s of our 59 calibrators, listed in Table 7. As the uncertainty of these absolute magnitudes depend not only on distance uncertainties, but also on extinction and reddening law uncertainties, we choose not to weigh the derived *PL* relations.

The adopted Galactic *PL* relations are given in Table 8: slope and intercept correspond to the relation $M = a \log P + b$. Their domain of validity extends from 0.57 to 1.65 in $\log P$ (3.7 to 45 days). We also define reddening-free Wesenheit magnitudes for the V and I_c bands, and similarly for the B and I_c bands, as:

$$W_{vi} = V - 2.55\,(V - I) \quad (1)$$

$$W_{bi} = B - 1.866\,(B - I) \quad (2)$$

where the colour coefficients are computed from the adopted reddening law (see Table 4). For the V and I_c bands, it is the same as the OGLE adopted coefficient (Udalski et al. 1999). The *PL* relations for these two Wesenheit magnitudes, which are less dispersed than the *PL* relations based on standard visible photometric bands, are also given in Table 8, and data are listed in Table 7.

Figures 2 and 3 display the adopted *PL* relations in the optical bands (B V R_c I_c W_{vi} and W_{bi}) and in the near-infrared (J H K_s), respectively.

4. Comparison of the Galactic and LMC *PL* relations

We will now compare our new Galactic *PL* relations to the LMC *PL* relations. The choice of the LMC *PL* relations in the visible is quite obvious, given the quality of the OGLE sample. The precise values of the slopes and intercepts of these relations depend on the adopted reddening corrections and on rejection of some outliers and of Cepheids with all kinds of imaginable problems (see Kanbur et al. 2003), as described in Fouqué et al. 2003. For simplicity, we will compare our results to the original OGLE relations from Udalski et al. (1999), as updated on the OGLE web site[4]: see Table 8.

In the infrared, we will use both the Persson et al. (2004) relations based on 92 Cepheids with well-sampled light curves (22 phase points per star on average), and an OGLE sample of 529 Cepheids ($0.4 < \log P < 1.5$) with 2MASS photometry from Soszyński et al. (2005), where the visible light curves have been used to transform the single-phase 2MASS measurements into mean magnitudes. We assume that LCO and 2MASS photometry are approximately in the same photometric system, which is confirmed by a direct comparison of 18 common stars, which shows an unsignificant shift of -0.02 ± 0.01 (in the sense Soszyński minus Persson) in all three bands. *PL* relations are given in Table 8.

In order to test for a possible change of slope at about a period of 10 days, as advocated for instance by Tammann et al. (2003) and Sandage et al. (2004), we enlarge the OGLE sample with 173 Cepheids from various sources, among which 68 have periods larger than 10 days. We are aware that adding these measurements from different photometric systems and with different assumed extinctions may well lead to the kind of systematic effects we want to test, so that, in our opinion, a superior way of

[4] ftp://sirius.astrouw.edu.pl/ogle/ogle2/var_stars/lmc/cep/catalog/README.PL.

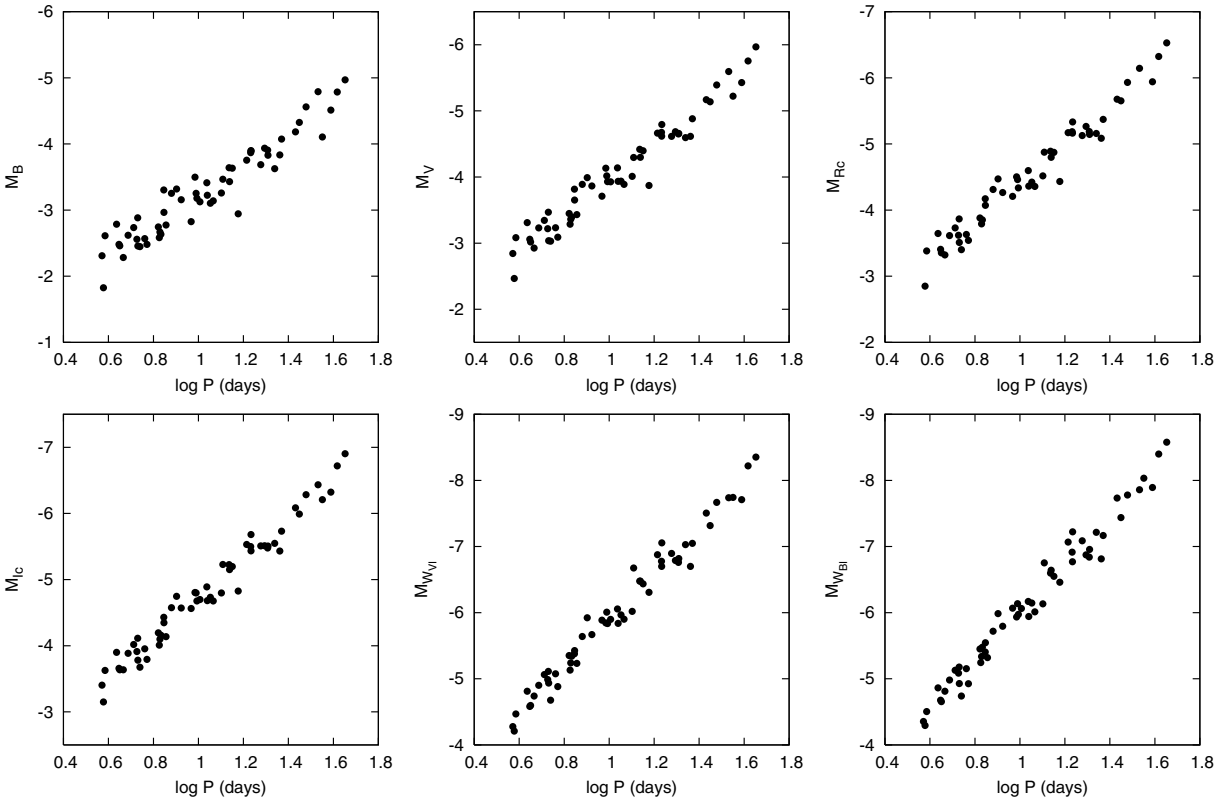

Fig. 2. Adopted Galactic *PL* relations in optical bands.

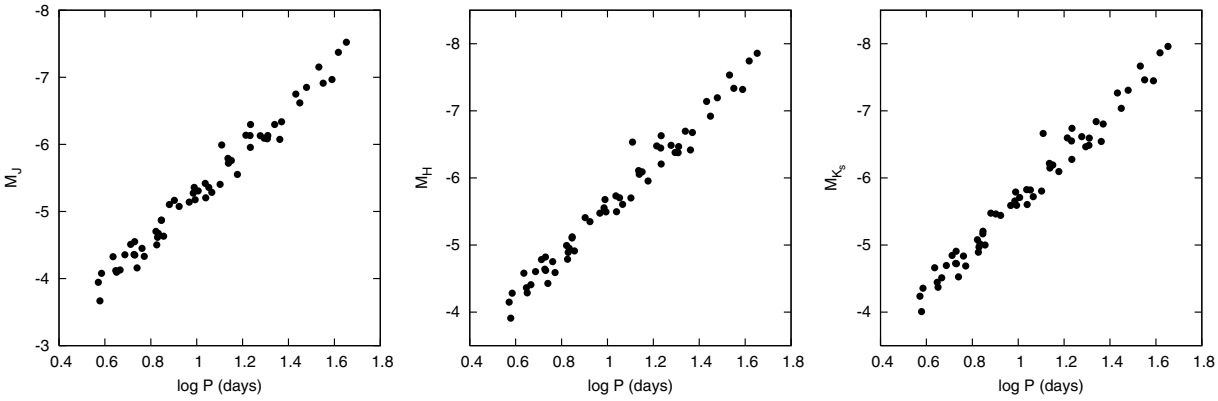

Fig. 3. Adopted Galactic *PL* relations in near-infrared bands.

definitively settling this important question will have to await for the publication of the OGLE shallow survey of LMC Cepheids. Optical photometry mainly comes from Sebo et al. (2002). We assume the same reddening law as for the Galactic Cepheids. Extinction values for this additional sample are adopted from Sandage et al. (2004) Table 1 (85 cases) and Gieren et al. (1998) Table 8 (KMS SW-341) when available, or assumed to be 0.1 if not (77 cases). The resulting *PL* relations in $B\ V\ R_c\ I_c$ are listed in Table 8. Six Cepheids with $\log P > 1.8$ have been a priori excluded from the sample. The final sample sizes after rejection of outliers are also listed in that table. Clearly, the new relations have a larger dispersion than the OGLE ones, probably because of a lower quality photometry and less accurate extinction values in the additional data. However, the slopes and intercepts are compatible within 1σ with the OGLE ones. The *PL* relations for the two Wesenheit magnitudes are also given in that Table. A comparison of these *PL* relations with original OGLE ones shows that adding long-period Cepheids does not change the *PL* relations significantly.

Comparison with the Galactic *PL* relations shows a general good agreement, except perhaps in W_{vi} and W_{bi}, where the Galactic slopes are slightly steeper. Small remaining differences in all bands may be due to the adopted slope of the *p (P)* relation, which is still uncertain. Good agreement can be judged in W_{vi} and K_s from Fig. 4, which displays Galactic data points together with LMC *PL* relations (from this work), using a magnitude offset of 18.40. This offset is the sum of the LMC distance modulus and any possible metallicity correction. As the same offset seems to work both in W_{vi} and K_s, possible metallicity corrections must be similar in both bands: for instance, negligible metallicity

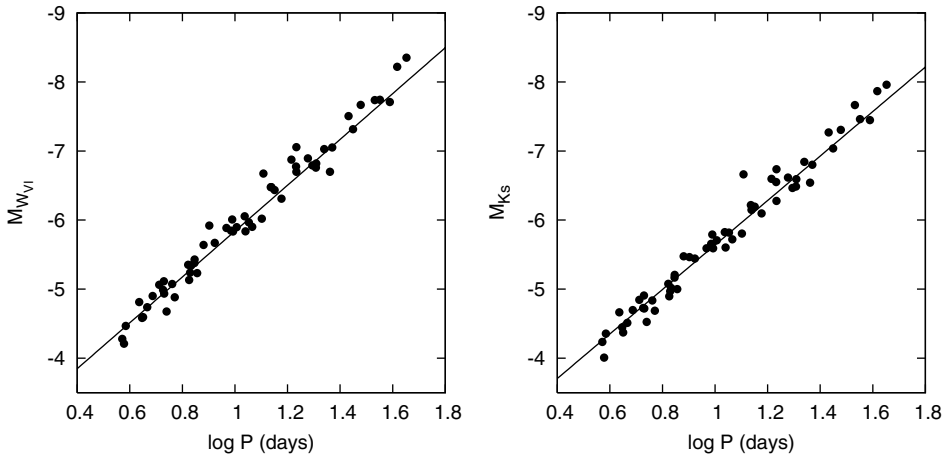

Fig. 4. Galactic *PL* relations in W_{vi} and K_s bands, superimposed with LMC Ogle relations shifted by a magnitude offset of 18.40.

correction in K and a correction of 0.13 mag in W_{vi}, as advocated by van Leeuwen et al. (2007), is in marginal disagreement with our findings. Moreover, as most published metallicity corrections are small and negative (which if true will make the more metal-poor LMC Cepheids intrinsically fainter, at a given period, than their Milky Way counterparts, implying a nearer LMC), and taking into account the dispersion of the Galactic data points, 18.50 appears to be an upper limit to the LMC distance modulus from our present study.

5. Summary and conclusion

The recent publication of accurate HST parallaxes of Galactic Cepheids has prompted new studies of the universality of the *PL* relations. However, the small number of measured Cepheids with this technique (10) does not allow an accurate determination of the slope of the Galactic *PL* relations. Similarly, the recent publication of revised Hipparcos parallaxes of Cepheids has the same limitation, because few Cepheids have a parallax accuracy better than 30%, and most of them are first overtone pulsators.

The main effort of the present study has been to increase the size of the sample of Galactic Cepheids with known parallaxes, using mainly the infrared surface brightness technique. Seventy Galactic Cepheids have now been measured by this method, among which 54 are suitable to calibrate the Galactic *PL* relations. We have chosen a recent determination of the *p (P)* relation based on hydrodynamical models to derive IRSB parallaxes. We verified that the HST parallaxes were compatible in the mean with these IRSB parallaxes. Adding five stars from other techniques, among which the interferometric Baade-Wesselink one, we are able to show that the Galactic slopes do not significantly differ from the corresponding slopes in the LMC for a given photometric band, from B to K.

This important result shows that applying the well determined LMC slopes to galaxies of different metallicity contents is warranted. Possible metallicity effects in the zero-point of the relations are not studied in the present work, and may still prevent a precise determination of galaxy distances using Cepheids. In the case of the LMC, the true distance modulus (corrected for metallicity effects) appears to be smaller than 18.50.

Acknowledgements. We express our gratitude to Leonid Berdnikov, John Caldwell, Michael Feast, Shashi Kanbur, Dave Laney, Chow Choong Ngeow, and Igor Soszyński for communicating unpublished data.

This publication makes use of data products from the 2MASS project, as well as the SIMBAD database, Aladin and Vizier catalogue operation tools (CDS Strasbourg, France). The Two Micron All Sky Survey is a joint project of the University of Massachusetts and the Infrared Processing and Analysis Center/California Institute of Technology, funded by the National Aeronautics and Space Administration and the National Science Foundation.

PA acknowledges the ALFA/LENAC network under the European Commission ALFA grant programme for financing her training at the Laboratoire d'Astrophysique de Toulouse.

This material is based in part upon work by TGB while serving at the National Science Foundation. Any opinions, findings, and conclusions or recommendations expressed in this material are those of the authors and do not necessarily reflect the views of the National Science Foundation.

WG acknowledges support for this work from the Chilean Center for Astrophysics FONDAP 15010003.

PF dedicates this work to Alain Milsztajn, who contributed to a better knowledge of Cepheids through the EROS survey, and passed away on June 28, 2007.

References

Barnes, III, T. G., Fernley, J. A., Frueh, M. L., et al. 1997, PASP, 109, 645
Barnes, III, T. G., Storm, J., Jefferys, W. H., Gieren, W. P., & Fouqué, P. 2005, ApJ, 631, 572
Benedict, G. F., McArthur, B. E., Fredrick, L. W., et al. 2002, AJ, 124, 1695
Benedict, G. F., McArthur, B. E., Feast, M. W., et al. 2007, AJ, 133, 1810
Berdnikov, L. N., Vozyakova, O. V., & Dambis, A. K. 1996a, Astron. Lett. 22, 334
Berdnikov, L. N., Vozyakova, O. V., & Dambis, A. K. 1996b, Astron. Lett. 22, 838
Berdnikov, L. N., Dambis, A. K., & Vozyakova, O. V. 2000, A&AS, 143, 211
Bersier, D. 1996, A&A, 308, 514
Bersier, D. 2002, ApJS, 140, 465
Bessell, M. S., Castelli, F., & Plez, B. 1998, A&A, 333, 231
Caldwell, J. A. R., & Coulson, I. M. 1987, AJ, 93, 1090
Cardelli, J. A., Clayton, G. C., & Mathis, J. S. 1989, ApJ, 345, 245
Carpenter, J. M. 2001, AJ, 121, 2851
Carroll, J. A. 1928, MNRAS, 88, 548
Claret, A. 2000, A&A, 363, 1081
Cohen, M., Wheaton, W. A., & Megeath, S. T. 2003, AJ, 126, 1090
Davis, J. 2006, Publ. Astron. Soc. Australia, 23, 94
Davis, J., Ireland, M. J., Jacob, A. P., et al. 2006, in Presented at the Society of Photo-Optical Instrumentation Engineers (SPIE) Conference, Advances in Stellar Interferometry, ed. J.D. Monnier, M. Schöller, & W.C. Danchi, Proc. SPIE, 6268, 626804
Dean, J. F. 1981, MNRAS, 197, 779
Dean, J. F., Warren, P. R., & Cousins, A. W. J. 1978, MNRAS, 183, 569
Eggen, O. J. 1996, AJ, 111, 1313
Feast, M. 1999, PASP, 111, 775
Feast, M. W., & Catchpole, R. M. 1997, MNRAS, 286, L1
Feltz, Jr., K. A., & McNamara, D. H. 1980, PASP, 92, 609
Fernie, J. D., Evans, N. R., Beattie, B., & Seager, S. 1995, Informational Bulletin on Variable Stars, 4148, 1
Fouqué, P., & Gieren, W. P. 1997, A&A, 320, 799

Fouqué, P., Storm, J., & Gieren, W. 2003, in Stellar Candles for the Extragalactic Distance Scale, ed. D. Alloin & W. Gieren, LNP, 635, 21
Gieren, W., Storm, J., Barnes, III, T. G., et al. 2005, ApJ, 627, 224
Gieren, W. P., Fouqué, P., & Gómez, M. 1998, ApJ, 496, 17
Groenewegen, M. A. T. 1999, A&AS, 139, 245
Groenewegen, M. A. T. 2004, MNRAS, 353, 903
Hindsley, R., & Bell, R. A. 1986, PASP, 98, 881
Hoyle, F., Shanks, T., & Tanvir, N. R. 2003, MNRAS, 345, 269
Janot-Pacheco, E. 1976, A&AS, 25, 159
Kanbur, S. M., Ngeow, C., Nikolaev, S., Tanvir, N. R., & Hendry, M. A. 2003, A&A, 411, 361
Kervella, P., Coudé du Foresto, V., Perrin, G., et al. 2001, A&A, 367, 876
Kervella, P., Bersier, D., Mourard, D., et al. 2004a, A&A, 428, 587
Kervella, P., Fouqué, P., Storm, J., et al. 2004b, ApJ, 604, L113
Kervella, P., Nardetto, N., Bersier, D., Mourard, D., & Coudé du Foresto, V. 2004c, A&A, 416, 941
Kervella, P., Mérand, A., Perrin, G., & Coudé Du Foresto, V. 2006, A&A, 448, 623
Kron, G. E., & Roach, F. E. 1979, in Changing Trends in Variable Star Research, ed. F. M. Bateson, J. Smak, & I. H. Urch, IAU Colloq., 46, 292
Lane, B. F., Kuchner, M. J., Boden, A. F., Creech-Eakman, M., & Kulkarni, S. R. 2000, Nature, 407, 485
Lane, B. F., Creech-Eakman, M. J., & Nordgren, T. E. 2002, ApJ, 573, 330
Laney, C. D., & Caldwell, J. A. R. 2007, MNRAS, 377, 147
Laney, C. D., & Stobie, R. S. 1992, A&AS, 93, 93
Laney, C. D., & Stobie, R. S. 1993, MNRAS, 263, 921
Marengo, M., Sasselov, D. D., Karovska, M., Papaliolios, C., & Armstrong, J. T. 2002, ApJ, 567, 1131
Marengo, M., Karovska, M., Sasselov, D. D., et al. 2003, ApJ, 589, 968
Mérand, A. 2008, in preparation
Mérand, A., Kervella, P., Coudé Du Foresto, V., et al. 2005, A&A, 438, L9
Mérand, A., Kervella, P., Coudé Du Foresto, V., et al. 2006, A&A, 453, 155
Mérand, A., Audenberg, J., Kervella, P., et al. 2007, [ArXiv.0704.1825]
Mourard, D., Bonneau, D., Koechlin, L., et al. 1997, A&A, 317, 789
Nardetto, N., Fokin, A., Mourard, D., et al. 2004, A&A, 428, 131
Nardetto, N., Mourard, D., Kervella, P., et al. 2006, A&A, 453, 309
Nardetto, N., Mourard, D., Mathias, P., Fokin, A., & Gillet, D. 2007, A&A, 471, 661
Nordgren, T. E., Armstrong, J. T., Germain, M. E., et al. 2000, ApJ, 543, 972
Nordgren, T. E., Lane, B. F., Hindsley, R. B., & Kervella, P. 2002, AJ, 123, 3380
Parsons, S. B. 1972, ApJ, 174, 57
Parsons, S. B., & Bell, R. A. 1975, Dudley Observatory Rep., 9, 73
Pel, J. W. 1978, A&A, 62, 75
Perryman, M. A. C., & ESA 1997, The Hipparcos and Tycho catalogues. Astrometric and photometric star catalogues derived from the ESA Hipparcos Space Astrometry Mission (Noordwijk, Netherlands: ESA Publications Division), ESA SP Ser., 1200
Persson, S. E., Madore, B. F., Krzemiński, W., et al. 2004, AJ, 128, 2239
Sandage, A., Tammann, G. A., & Reindl, B. 2004, A&A, 424, 43
Schechter, P. L., Avruch, I. M., Caldwell, J. A. R., & Keane, M. J. 1992, AJ, 104, 1930
Sebo, K. M., Rawson, D., Mould, J., et al. 2002, ApJS, 142, 71
Skrutskie, M. F., Cutri, R. M., Stiening, R., et al. 2006, AJ, 131, 1163
Soderblom, D. R., Nelan, E., Benedict, G. F., et al. 2005, AJ, 129, 1616
Soszyński, I., Gieren, W., & Pietrzyński, G. 2005, PASP, 117, 823
Storm, J., Barnes, III, T. G., Jefferys, W. H., Fouqué, P., & Gieren, W. P. 2008, in preparation
Tammann, G. A., Sandage, A., & Reindl, B. 2003, A&A, 404, 423
Turner, D. G., & Burke, J. F. 2002, AJ, 124, 2931
Turner, D. G., Leonard, P. J. T., & English, D. A. 1987, AJ, 93, 368
Udalski, A., Szymanski, M., Kubiak, M., et al. 1999, Acta Astron., 49, 201
van Leeuwen, F., Feast, M. W., Whitelock, P. A., & Laney, C. D. 2007, [ArXiv:0705.1592]
Welch, D. L., Wieland, F., McAlary, C. W., et al. 1984, ApJS, 54, 547
Yakimova, N. N., Nikolov, N. S., & Ivanov, G. R. 1975, in Variable Stars and Stellar Evolution, ed. V. E. Sherwood & L. Plaut, IAU Symp., 67, 201

Online Material

Table 2. Adopted weighted mean extinction values for the 155 Cepheids in Laney & Caldwell (2007), GT Car, SU Cru and BG Cru.

Star	$E(B-V)$	m.e.	N	Star	$E(B-V)$	m.e.	N	Star	$E(B-V)$	m.e.	N
U Aql	0.360	0.010	10	X Cyg	0.228	0.012	9	X Pup	0.402	0.009	10
SZ Aql	0.537	0.017	9	SU Cyg	0.098	0.014	4	RS Pup	0.457	0.009	10
TT Aql	0.438	0.011	8	SZ Cyg	0.571	0.015	5	VZ Pup	0.459	0.011	7
FF Aql	0.196	0.010	8	TX Cyg	1.130	0.015	5	WX Pup	0.301	0.015	4
FM Aql	0.589	0.012	9	VY Cyg	0.606	0.019	3	WZ Pup	0.227	0.016	4
FN Aql	0.483	0.010	7	VZ Cyg	0.266	0.011	6	AQ Pup	0.518	0.010	8
V496 Aql	0.397	0.010	7	CD Cyg	0.493	0.015	5	AT Pup	0.191	0.010	8
V600 Aql	0.798	0.016	4	DT Cyg	0.042	0.011	7	BN Pup	0.416	0.018	3
η Aql	0.130	0.009	13	MW Cyg	0.635	0.017	4	LS Pup	0.461	0.015	4
RT Aur	0.059	0.013	5	V386 Cyg	0.841	0.017	4	S Sge	0.100	0.010	9
RX Aur	0.263	0.012	5	V402 Cyg	0.391	0.025	2	GY Sge	1.187	0.170	2
RW Cam	0.633	0.016	4	V459 Cyg	0.730	0.019	3	U Sgr	0.403	0.009	12
RX Cam	0.532	0.011	7	V532 Cyg	0.494	0.015	5	W Sgr	0.108	0.011	6
RY CMa	0.239	0.010	7	V924 Cyg	0.261	0.025	2	X Sgr	0.237	0.015	9
RZ CMa	0.443	0.016	4	V1726 Cyg	0.339	0.058	2	Y Sgr	0.191	0.010	8
SS CMa	0.553	0.011	8	β Dor	0.052	0.010	9	WZ Sgr	0.431	0.011	8
TW CMa	0.329	0.016	4	W Gem	0.255	0.010	8	XX Sgr	0.521	0.017	4
U Car	0.265	0.010	8	RZ Gem	0.563	0.026	4	YZ Sgr	0.281	0.010	7
V Car	0.169	0.011	6	AA Gem	0.309	0.017	4	AP Sgr	0.178	0.010	7
SX Car	0.318	0.015	4	AD Gem	0.173	0.019	3	BB Sgr	0.281	0.009	10
UX Car	0.112	0.012	7	DX Gem	0.430	0.015	4	V350 Sgr	0.299	0.010	8
VY Car	0.237	0.009	9	ζ Gem	0.014	0.011	7	RV Sco	0.349	0.010	9
WZ Car	0.370	0.011	8	V Lac	0.335	0.017	4	RY Sco	0.718	0.018	6
XX Car	0.347	0.012	6	X Lac	0.336	0.011	7	KQ Sco	0.869	0.021	5
XY Car	0.411	0.014	5	Y Lac	0.207	0.016	4	V482 Sco	0.336	0.013	6
XZ Car	0.365	0.010	8	Z Lac	0.370	0.011	7	V500 Sco	0.593	0.016	4
YZ Car	0.381	0.012	6	RR Lac	0.319	0.014	6	Y Sct	0.757	0.012	7
AQ Car	0.165	0.012	6	BG Lac	0.300	0.016	4	Z Sct	0.492	0.013	6
CT Car	0.570	0.025	2	GH Lup	0.335	0.018	3	RU Sct	0.921	0.012	7
FR Car	0.334	0.014	5	T Mon	0.181	0.011	12	SS Sct	0.325	0.010	8
GI Car	0.200	0.011	6	SV Mon	0.234	0.010	8	CM Sct	0.721	0.019	3
GT Car	0.866	0.029	1	TX Mon	0.485	0.013	6	EV Sct	0.655	0.013	8
ℓ Car	0.147	0.013	8	CS Mon	0.506	0.018	3	V367 Sct	1.231	0.025	2
RW Cas	0.380	0.019	5	CV Mon	0.722	0.022	7	BQ Ser	0.815	0.025	2
SU Cas	0.259	0.010	9	S Mus	0.212	0.017	7	ST Tau	0.368	0.031	3
SW Cas	0.467	0.019	3	RT Mus	0.344	0.021	6	SZ Tau	0.295	0.011	6
SZ Cas	0.794	0.013	4	UU Mus	0.399	0.015	4	R TrA	0.142	0.010	8
CF Cas	0.553	0.011	7	S Nor	0.179	0.009	10	S TrA	0.084	0.009	10
DD Cas	0.450	0.017	4	U Nor	0.862	0.024	8	α UMi	0.003	0.013	6
DL Cas	0.488	0.010	9	TW Nor	1.157	0.014	4	T Vel	0.289	0.010	8
FM Cas	0.325	0.017	4	QZ Nor	0.253	0.016	4	V Vel	0.186	0.019	6
V Cen	0.292	0.012	9	V340 Nor	0.321	0.018	3	RY Vel	0.547	0.010	9
VW Cen	0.428	0.024	6	Y Oph	0.645	0.015	9	RZ Vel	0.299	0.010	8
XX Cen	0.266	0.011	6	BF Oph	0.235	0.010	7	SW Vel	0.344	0.010	9
AZ Cen	0.168	0.010	8	RS Ori	0.352	0.012	7	SX Vel	0.263	0.012	5
KN Cen	0.797	0.091	6	GQ Ori	0.249	0.014	5	AX Vel	0.224	0.012	5
V339 Cen	0.413	0.014	5	SV Per	0.408	0.019	5	CS Vel	0.737	0.029	4
CR Cep	0.709	0.017	4	UY Per	0.873	0.011	6	DR Vel	0.656	0.014	5
δ Cep	0.075	0.010	9	VX Per	0.475	0.011	7	S Vul	0.727	0.042	3
S Cru	0.166	0.010	8	VY Per	0.945	0.013	6	T Vul	0.064	0.011	7
SU Cru	0.942	0.096	5	AS Per	0.674	0.019	3	U Vul	0.603	0.011	6
AG Cru	0.212	0.018	5	AW Per	0.489	0.012	6	X Vul	0.742	0.019	7
BG Cru	0.132	0.023	4					SV Vul	0.461	0.022	8

Table 6. Adopted parallax of our calibrators. Five different distance indicators have been considered, but only one has been chosen: HST (1), IBW (2), IRSB (3), ZAMS (4), HIP (5). Last column lists the available indicators, the first one being the adopted one. When a distance indicator is of low quality or leads to rejection, it is given in brackets. FO marks the stars suspected to pulse in the first overtone mode. DM means double mode pulsator.

Star	log P	π	$\sigma(\pi)$	source	mode	Star	log P	π	$\sigma(\pi)$	source	mode
U Aql	0.846591	1.65	0.08	3		S Nor	0.989194	1.06	0.05	34	
SZ Aql	1.234029	0.46	0.01	3		U Nor	1.101875	0.81	0.04	3	
TT Aql	1.138459	0.99	0.03	3		TW Nor	1.0329	0.52	0.03	4	
FF Aql	0.650397	2.81	0.18	15(3)		QZ Nor	0.578244	0.79	0.10	34	
FM Aql	0.786342	0.85	0.05	(3)		V340 Nor	1.052579	0.56	0.11	34	
FN Aql	0.976878	0.90	0.03	(3)		Y Oph	1.233609	1.81	0.13	32	
V496 Aql	0.832958	1.07	0.11	3		BF Oph	0.609329	1.57	0.08	(3)	
η Aql	0.855930	4.15	0.24	325		X Pup	1.4143	0.47	0.03	(3)	
RT Aur	0.571489	2.40	0.19	1(35)		RS Pup	1.617420	0.55	0.03	34	
U Car	1.588970	0.67	0.03	34		VZ Pup	1.364945	0.27	0.02	(3)	
V Car	0.82586	0.96	0.14	3		AQ Pup	1.478624	0.33	0.02	3(4)	
VY Car	1.276818	0.55	0.03	34		BN Pup	1.135867	0.26	0.02	3	
WZ Car	1.361977	0.29	0.01	3		LS Pup	1.150646	0.21	0.02	3	
GT Car	1.119	0.10	0.02	(4)		S Sge	0.923352	1.48	0.05	3	
ℓ Car	1.550816	2.01	0.20	1235		GY Sge	1.7081	0.32	0.01	(34)	
SU Cas	0.289884	2.25	0.17	354	FO	U Sgr	0.828997	1.77	0.06	34	
CF Cas	0.6880	0.29	0.02	4		W Sgr	0.880522	2.28	0.20	15(2)	
DL Cas	0.9031	0.60	0.03	4		X Sgr	0.845907	3.00	0.18	15	
V Cen	0.739882	1.65	0.12	34		Y Sgr	0.761428	2.13	0.29	13(25)	
VW Cen	1.177138	0.28	0.01	3		WZ Sgr	1.339443	0.57	0.02	34	
XX Cen	1.039548	0.66	0.04	3		YZ Sgr	0.980171	1.00	0.12	(3)	
KN Cen	1.531857	0.27	0.02	3		BB Sgr	0.821971	1.27	0.05	34	
δ Cep	0.729678	3.66	0.15	1235(4)		V350 Sgr	0.712165	1.07	0.06	3	
SU Cru	1.1088	0.62	0.08	3		RY Sco	1.307927	0.85	0.04	3	
BG Cru	0.524	2.23	0.30	5	FO	KQ Sco	1.4577	0.35	0.04	4	
X Cyg	1.214482	0.86	0.02	34		RU Sct	1.29448	0.58	0.05	34	
SU Cyg	0.584952	1.19	0.05	34		SS Sct	0.564814	1.32	0.15	(3)	
VZ Cyg	0.687034	0.54	0.02	3		EV Sct	0.490098	0.60	0.12	(3)4	FO
CD Cyg	1.232334	0.39	0.01	3		V367 Sct	0.7989	0.61	0.03	4	DM
DT Cyg	0.397804	2.19	0.33	5(3)	FO	SZ Tau	0.498166	1.95	0.11	345	FO
β Dor	0.993131	3.14	0.16	135(2)		α UMi	0.5990	7.72	0.12	5	FO
ζ Gem	1.006507	2.78	0.18	1245		T Vel	0.666501	0.99	0.01	3	
X Lac	0.735997	0.37	0.05	3	FO	RY Vel	1.449158	0.45	0.03	3	
Y Lac	0.635863	0.44	0.02	3		RZ Vel	1.309564	0.70	0.03	345	
Z Lac	1.036854	0.53	0.01	3		SW Vel	1.370016	0.42	0.01	34	
BG Lac	0.726883	0.59	0.03	3		CS Vel	0.771201	0.33	0.03	34	
GH Lup	0.967448	0.89	0.15	3		S Vul	1.837426	0.24	0.09	(34)	
T Mon	1.431915	0.72	0.03	34		T Vul	0.646934	1.90	0.23	135	
CV Mon	0.730685	0.63	0.05	34		U Vul	0.902584	1.46	0.06	3	
S Mus	0.98498	1.22	0.08	35		SV Vul	1.652569	0.46	0.01	34	
UU Mus	1.065819	0.33	0.04	3							

Table 7. Adopted absolute magnitudes of the 59 calibrators in 7 photometric bands (from B to K_s) and for two Wesenheit indices, W_{vi} and W_{bi}.

Star	log P	M_B	M_V	M_{Rc}	M_{Ic}	M_{Wvi}	M_{Wbi}	M_J	M_H	M_{Ks}
RT Aur	0.571489	–2.31	–2.84		–3.40	–4.28	–4.35	–3.94	–4.15	–4.24
QZ Nor	0.578244	–1.83	–2.47	–2.85	–3.15	–4.21	–4.29	–3.67	–3.91	–4.01
SU Cyg	0.584952	–2.61	–3.08	–3.38	–3.63	–4.47	–4.50	–4.08	–4.28	–4.36
Y Lac	0.635863	–2.79	–3.31	–3.65	–3.90	–4.81	–4.86	–4.33	–4.58	–4.66
T Vul	0.646934	–2.48	–3.06	–3.41	–3.66	–4.58	–4.68	–4.12	–4.36	–4.45
FF Aql	0.650397	–2.46	–3.02	–3.35	–3.64	–4.60	–4.65	–4.09	–4.29	–4.37
T Vel	0.666501	–2.28	–2.93	–3.32	–3.64	–4.74	–4.81	–4.13	–4.41	–4.51
VZ Cyg	0.687034	–2.62	–3.23	–3.62	–3.88	–4.90	–4.98	–4.36	–4.60	–4.70
V350 Sgr	0.712165	–2.74	–3.34	–3.73	–4.02	–5.06	–5.13	–4.51	–4.78	–4.85
BG Lac	0.726883	–2.56	–3.22	–3.62	–3.91	–4.99	–5.08	–4.36	–4.64	–4.73
δ Cep	0.729678	–2.88	–3.47	–3.87	–4.11	–5.11	–5.18	–4.55	–4.82	–4.91
CV Mon	0.730685	–2.46	–3.04	–3.51	–3.78	–4.94	–4.93	–4.35	–4.62	–4.72
V Cen	0.739882	–2.45	–3.03	–3.40	–3.68	–4.68	–4.74	–4.16	–4.43	–4.52
Y Sgr	0.761428	–2.57	–3.23	–3.63	–3.95	–5.07	–5.15	–4.45	–4.75	–4.83
CS Vel	0.771201	–2.48	–3.09	–3.54	–3.79	–4.88	–4.93	–4.33	–4.59	–4.69
BB Sgr	0.821971	–2.74	–3.45	–3.88	–4.19	–5.35	–5.45	–4.70	–4.99	–5.08
V Car	0.82586	–2.58	–3.29		–4.01	–5.13	–5.24	–4.50	–4.79	–4.89
U Sgr	0.828997	–2.67	–3.36	–3.79	–4.10	–5.24	–5.34	–4.61	–4.89	–4.97
V496 Aql	0.832958	–2.63	–3.39	–3.85	–4.16	–5.34	–5.48	–4.67	–4.95	–5.02
X Sgr	0.845907	–3.31	–3.82	–4.17	–4.43	–5.38	–5.40	–4.87	–5.10	–5.17
U Aql	0.846591	–2.97	–3.65	–4.07	–4.35	–5.43	–5.55	–4.87	–5.12	–5.21
η Aql	0.855930	–2.77	–3.43		–4.14	–5.23	–5.32	–4.63	–4.91	–5.00
W Sgr	0.880522	–3.25	–3.89	–4.31	–4.58	–5.64	–5.72	–5.10		–5.47
U Vul	0.902584	–3.32	–3.99	–4.47	–4.75	–5.92	–5.99	–5.17	–5.41	–5.46
S Sge	0.923352	–3.16	–3.86	–4.27	–4.57	–5.67	–5.79	–5.07	–5.35	–5.44
GH Lup	0.967448	–2.83	–3.71	–4.21	–4.56	–5.88	–6.07	–5.14	–5.47	–5.59
S Mus	0.98498	–3.50	–4.13	–4.50	–4.80	–5.85	–5.93	–5.27	–5.55	–5.66
S Nor	0.989194	–3.25	–4.02	–4.46	–4.80	–6.01	–6.14	–5.36	–5.68	–5.79
β Dor	0.993131	–3.18	–3.93	–4.34	–4.68	–5.84	–5.97	–5.17	–5.49	–5.59
ζ Gem	1.006507	–3.13	–3.93		–4.70	–5.90	–6.06	–5.31		–5.71
Z Lac	1.036854	–3.41	–4.14	–4.60	–4.89	–6.06	–6.17	–5.42	–5.73	–5.83
XX Cen	1.039548	–3.22	–3.93	–4.36	–4.68	–5.84	–5.94	–5.20	–5.50	–5.60
V340 Nor	1.052579	–3.10	–3.94	–4.42	–4.73	–5.97	–6.14	–5.36	–5.70	–5.82
UU Mus	1.065819	–3.14	–3.89	–4.36	–4.68	–5.90	–6.01	–5.29	–5.60	–5.72
U Nor	1.101875	–3.26	–4.01	–4.52	–4.80	–6.02	–6.13	–5.40	–5.70	–5.80
SU Cru	1.1088	–3.47	–4.30	–4.88	–5.23	–6.67	–6.75	–5.99	–6.53	–6.66
BN Pup	1.135867	–3.64	–4.42	–4.89	–5.23	–6.48	–6.60	–5.79	–6.11	–6.22
TT Aql	1.138459	–3.43	–4.30	–4.80	–5.15	–6.48	–6.64	–5.72	–6.05	–6.15
LS Pup	1.150646	–3.63	–4.40	–4.87	–5.20	–6.44	–6.55	–5.76	–6.09	–6.19
VW Cen	1.177138	–2.94	–3.87	–4.43	–4.83	–6.31	–6.46	–5.55	–5.95	–6.10
X Cyg	1.214482	–3.76	–4.66	–5.17	–5.53	–6.88	–7.07	–6.14	–6.48	–6.60
CD Cyg	1.232334	–3.87	–4.68	–5.19	–5.50	–6.78	–6.91	–6.13	–6.45	–6.55
Y Oph	1.233609	–3.89	–4.62	–5.16	–5.43	–6.70	–6.77	–5.96	–6.21	–6.28
SZ Aql	1.234029	–3.90	–4.79	–5.33	–5.68	–7.05	–7.22	–6.30	–6.63	–6.74
VY Car	1.276818	–3.69	–4.61	–5.13	–5.51	–6.89	–7.09	–6.13	–6.49	–6.61
RU Sct	1.29448	–3.94	–4.69	–5.26	–5.51	–6.79	–6.87	–6.09	–6.38	–6.46
RY Sco	1.307927	–3.91	–4.65	–5.19	–5.48	–6.76	–6.84	–6.09	–6.38	–6.49
RZ Vel	1.309564	–3.83	–4.66	–5.14	–5.51	–6.82	–6.96	–6.13	–6.47	–6.59
WZ Sgr	1.339443	–3.63	–4.60	–5.16	–5.55	–7.03	–7.21	–6.30	–6.70	–6.84
WZ Car	1.361977	–3.83	–4.61	–5.09	–5.43	–6.70	–6.81	–6.08	–6.42	–6.54
SW Vel	1.370016	–4.07	–4.88	–5.37	–5.73	–7.05	–7.17	–6.34	–6.68	–6.80
T Mon	1.431915	–4.18	–5.17	–5.68	–6.08	–7.51	–7.73	–6.75	–7.14	–7.27
RY Vel	1.449158	–4.32	–5.14	–5.65	–5.99	–7.32	–7.44	–6.62	–6.92	–7.04
AQ Pup	1.478624	–4.56	–5.39	–5.93	–6.28	–7.67	–7.78	–6.85	–7.20	–7.31
KN Cen	1.531857	–4.79	–5.59	–6.14	–6.43	–7.74	–7.86	–7.15	–7.53	–7.67
ℓ Car	1.550816	–4.11	–5.22		–6.21	–7.74	–8.03	–6.91	–7.33	–7.46
U Car	1.588970	–4.51	–5.43	–5.94	–6.32	–7.71	–7.89	–6.97	–7.32	–7.45
RS Pup	1.617420	–4.78	–5.76	–6.32	–6.72	–8.22	–8.40	–7.37	–7.74	–7.87
SV Vul	1.652569	–4.97	–5.97	–6.53	–6.90	–8.35	–8.58	–7.52	–7.86	–7.96